

Review

A Review of Crystalline Multibridged Cyclophane Cages: Synthesis, Their Conformational Behavior, and Properties

 Xing-Xing Zhang ¹, Jian Li ² and Yun-Yin Niu ^{1,*} 
¹ Green Catalysis Center, College of Chemistry, Zhengzhou University, No. 100 Science Avenue, Zhengzhou 450001, China

² College of Ecology and Environment, Zhengzhou University, Zhengzhou 450001, China

* Correspondence: niuyy@zzu.edu.cn

Abstract: This paper reviews the most stable conformation of crystalline three-dimensional cyclophane (CP) achieved by self-assembling based on changing the type of aromatic compound or regulating the type and number of bridging groups. [3_n]cyclophanes (CPs) were reported to form supramolecular compounds with bind organic, inorganic anions, or neutral molecules selectively. [3_n]cyclophanes ([3_n]CPs) have stronger donor capability relative to compound [2_n]cyclophanes ([2_n]CPs), and it is expected to be a new type of electron donor for the progress of fresh electron conductive materials. The synthesis, conformational behavior, and properties of crystalline multi-bridge rings are summarized and discussed.

Keywords: cyclophane; conformation; supramolecule; 3D molecule; NHC carbene; review



Citation: Zhang, X.-X.; Li, J.; Niu, Y.-Y. A Review of Crystalline Multibridged Cyclophane Cages: Synthesis, Their Conformational Behavior, and Properties. *Molecules* **2022**, *27*, 7083. <https://doi.org/10.3390/molecules27207083>

Academic Editor: Miroslaw Jablonski

Received: 24 September 2022

Accepted: 17 October 2022

Published: 20 October 2022

Publisher's Note: MDPI stays neutral with regard to jurisdictional claims in published maps and institutional affiliations.



Copyright: © 2022 by the authors. Licensee MDPI, Basel, Switzerland. This article is an open access article distributed under the terms and conditions of the Creative Commons Attribution (CC BY) license (<https://creativecommons.org/licenses/by/4.0/>).

1. Introduction

Supramolecular chemistry was first proposed by the “Father of Supramolecular Chemistry” Lehn based on Pedersen’s study of crown ethers [1–4], it is mainly the science of studying the system with specific functions formed by chemical substances through the intermolecular force of noncovalent bonds [5,6]. As an interdisciplinary subject, supramolecular science has made remarkable achievements in recent years [7,8]. It has great application potential in the fields of life science, environmental science, materials science, energy science, and medical science [9,10]. The designs and synthesis of artificial organic macrocyclic compounds with molecular recognition ability are one of the research hotspots in supramolecular chemistry [11,12]. As artificial receptors, cyclophanes are macrocyclic compounds formed by bridging multiple aromatic compounds [13,14]. By changing the type of aromatic compounds or regulating the type and quantity of bridging groups [15], cyclophanes are endowed with new self-assembly strategies and physical-chemical synergistic driving forces such as hydrogen bond, electrostatic interaction, hydrophobic interaction, π - π bond, metal ion coordination and so on [16–18]. Therefore, cyclophane and its derivatives, including crown ether, cyclodextrin, and calixarene, are becoming a very important class of host compounds in supramolecular chemistry [19–24]. Because cyclophane has multiple active sites and a unique cavity structure, it can selectively recognize guest molecules or ions [25–30]. It also has many properties such as optical properties, catalytic activity and drug activity [31,32], which gives it broad application prospects in the fields of chemical battery [33,34], electrochemical sensor [35], biomedical, [31] material science [36] and so on.

The term multiple-bridged cyclophane is understood to denote those with more than two bridges, as commonly used by [m_n]cyclophane (m = n = 3–6) (Figure 1) to indicate poly bridge cyclophane, for example, [2_n]CPs contain two benzene rings and three to six ethanol bridges and [3_n]CPs contain two benzene rings and three to six propane bridges. Figure 2 shows the structural diagrams of [3₃](1,3,5)CP, [3₄](1,2,4,5)CP, [3₄](1,2,3,5)CP, [3₅](1,2,3,4,5)CP, [3₆](1,2,3,4,5,6)CP [37], which look like some pinwheels with different

blades [38,39]. In recent decades, with the synthesis of a large number of artificial cyclophanes [40–43], two-dimensional (2D) and three-dimensional (3D) multiple-bridged cyclophanes have a wide development trend and are widely used in the field of artificial macrocyclic compounds [44]. In the artificial bionic simulation experiment, it largely depends on whether an efficient active cage can be constructed and whether the main molecules with specific active cavities can be designed and synthesized [45–47]. Compared with two-dimensional planar cyclophane, three-dimensional cyclophane can build catalytic cages and form more valuable simulation systems, which is of great significance not only for the selective recognition of anions, amphoteric molecules, and other substances [48–50], but also for the catalysis of supramolecule [51]. Therefore, this review is based on the summary and progress of three-dimensional cyclophanes [52]. The focus is especially on the three-dimensional cyclophane cages in the crystalline state because the crystalline material has special properties such as anisotropy, definite melting point, and X-ray diffraction compared with the amorphous material [53,54].

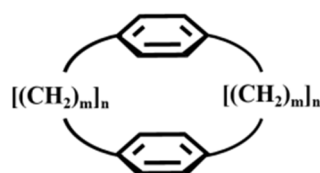


Figure 1. The structure diagram of $[m_n]$ cyclophane ($m = n = 3–6$).

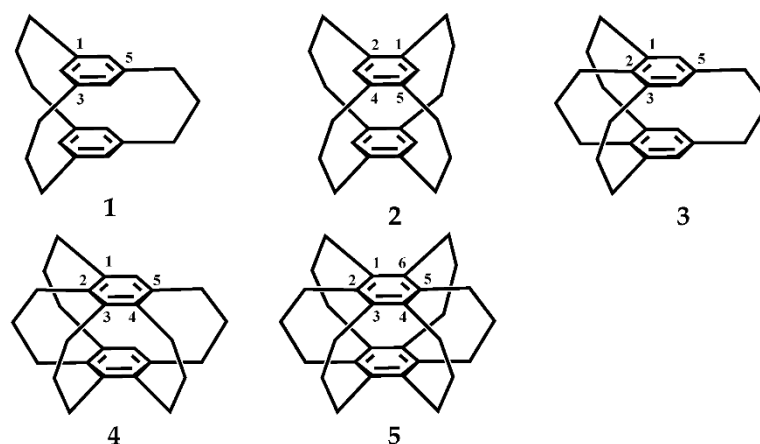


Figure 2. The structure diagrams of $[3_3](1,3,5)$ CP 1, $[3_4](1,2,4,5)$ CP 2, $[3_4](1,2,3,5)$ CP 3, $[3_5](1,2,3,4,5)$ CP 4, and $[3_6](1,2,3,4,5,6)$ CP 5.

2. Results and Discussion

2.1. Crystalline Three-Fold Bridged Cyclophanes

2.1.1. Carbon Chain Three-Bridge Cage

Carbon chain three-bridge cyclophanes $[3_n]$ CPs are flowing in solution, and among them, the flip process of Sanya methyl bridges causes their conformational isomerism. The most secure conformers are summed up in Figure 3 [37].

By making use of the strong ability of $[3_n]$ CPs to give electrons, Mikio et al. synthesized the CT (charge-transfer) compounds with TCNE (tetracyanoethylene), TCNQ (Tetracyanoquinodimethane), and TCNQ-F4. $[3_3](1,3,5)$ CP-TCNE (1:1) compound 6 (Figure 4) was synthesized at $-180\text{ }^\circ\text{C}$ [37]. In its crystal structure, each TCNE was arranged as a sandwich between two cyclophane molecules, located on or near the center of symmetry, which resulted in a compound (1:1) with alternating D-A stacking. The benzene ring in the compound is almost parallel to the TCNE molecule and the average distance between plane-to-plane is 3.22 \AA . The average transannular distance between the two benzene rings

is 3.11 Å (Figure 5). $[3_3](1,3,5)\text{CP-TCNQ}$ complex 7 (Figure 4) was obtained as two crystalline modifications. 7 (2:1) as prisms were synthesized from $\text{CH}_3\text{CN-CH}_2\text{Cl}_2$ at -180°C , whereas 7 (4:1) as plates were synthesized from $\text{MeOH-CH}_2\text{Cl}_2$ at -180°C . In the crystal structure of 7 (2:1), a TCNQ and a cyclophane are superimposed. In addition, the benzene ring and the TCNQ of the cyclophane partially overlap, a cyclophane and a TCNQ are stacked with the D-A distance being 3.26 Å. The average transannular distance between these two benzene rings is 3.12 Å (Figure 5). Because of the disorder of the molecule, cyclophanes are found to have two conformations: C_s and C_{3h} . Each cyclophane interacts with TCNQ on only one surface of the molecule. The final consequence is that two cyclophanes are coordinated to one TCNQ. In the crystal structure of 7 (4:1), a similar D-A overlap was found in a TCNQ and cyclophane, and 3.39 Å is their D-A distance. By the force of $\text{CH-}\pi$, the other naphthene interacts (2.90 Å) with an alkene proton of TCNQ to form a 4:1 unit (Figure 5). In the crystal structure, the cyclophane moiety of $[3_3](1,3,5)\text{CP-TCNQ-F4}$ (1:1) complex 8 (Figure 4) is C_s . The D-A overlapping pattern is semblable to that of 7, and 3.32 Å is the transannular D-A distance. Sectional overlapping receptors are regularly stacked with a distance of 2.93 Å in infinite columns (Figure 5). By contrast, it is possible that complex 8 has an infinite column of partially overlapping receptors with short A-A distances, and that receptors arranged parallel to each other in the plane of the unit cell are in close contact. Resulting in greater charge separation, making it more conductive.

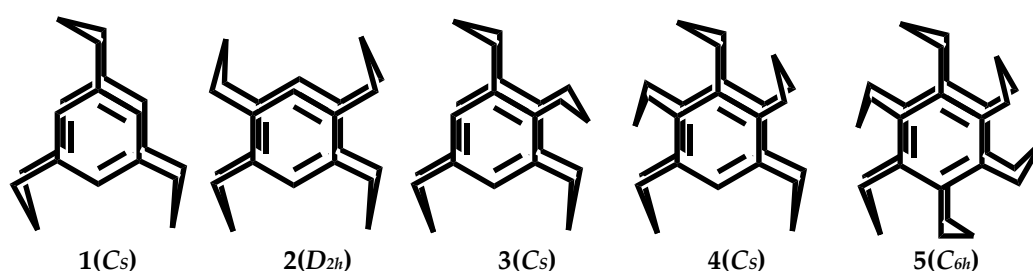


Figure 3. The most secure conformers of multibridged $[3_n]\text{CPs}$ ($n = 3-6$).

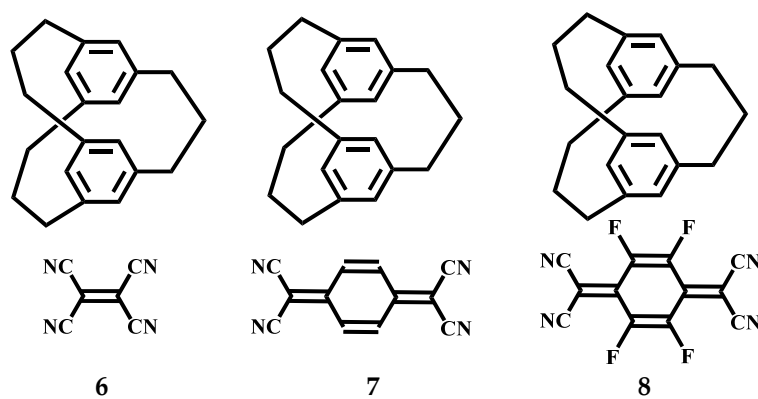


Figure 4. The structures of $[3_3]\text{CPs-TCNE}$, $-TCNQ$, and $-TCNQ-F4$ complexes 6, 7, and 8.

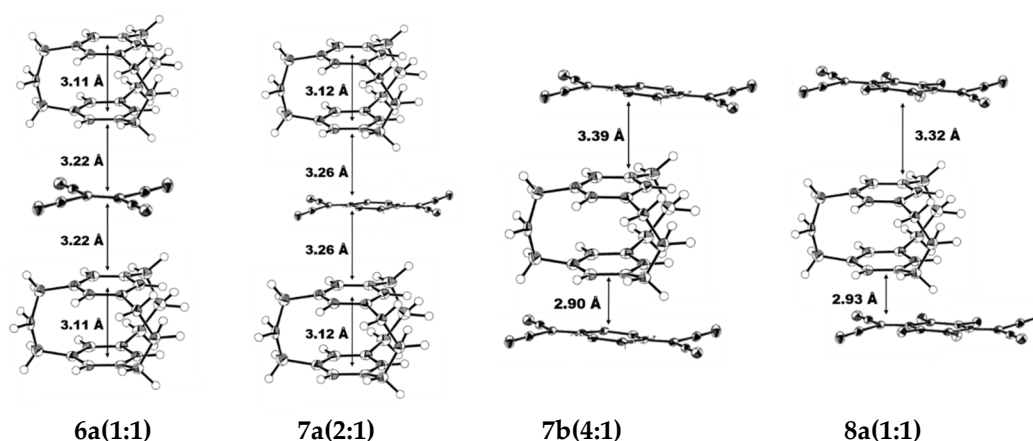


Figure 5. ORTEP drawings of complexes 6, 7, and 8 at $-180\text{ }^{\circ}\text{C}$ (the probability of thermal ellipsoid is 50%).

Mikio et al. studied the solid-state structure of the Charge-Transfer Complexes of 5,7,9-Trimethyl and 2,11,20-Trithia $[3_3](1,3,5)$ CPs [55]. $\text{Me}_3[3_3]$ CP exists in the C_3 conformation in both solid and liquid states, with three bridges pointing in either clockwise or counterclockwise directions. Under the reaction at $-170\text{ }^{\circ}\text{C}$, two types of D-A overlap were found in crystals of $\text{Me}_3[3_3](1,3,5)$ CP-TCNQ-F4 (1:1) complex 9 (Figure 6). One is attributed to efficient HOMO-LUMO orbital interaction, with a partial D-A overlap of the methyl-substituted benzene ring and TCNQ-F4 in the $[3_3](1,3,5)$ CP-TCNQ-F4 complex. In contrast, the methyl-unsubstituted benzene ring is almost completely overlapped with TCNQ-F4. The cross-ring D-A distance of the former (3.22 Å) is much shorter than the cross-ring D-A distance of the latter (3.58 Å), which illustrates the view that the methyl-substituted benzene ring interacts more strongly with the acceptor than the methyl-unsubstituted benzene ring (Figure 7). Recipients and donors are stacked alternately, and the transannular distance between recipients is 3.26 Å on the methyl-substituted side and 3.45 Å on the methyl-unsubstituted side (Figure 7). Under the reaction at $-170\text{ }^{\circ}\text{C}$, C_s structure was observed in the cyclophane portion of $\text{S}_3[3_3](1,3,5)$ CP-TCNQ-F4 (1:1) complex 10 (Figure 6). The cross-ring D-A distance is 3.29 Å, and the average cross-ring distance between two benzene rings is 3.23 Å (Figure 7). Among them, partially overlapping receptors form an infinite column, and the distance between receptors is 3.10 Å, which is larger than that of complex 8 (2.93 Å), which is attributed to the weaker donation ability of $\text{S}_3[3_3](1,3,5)$ CP than $[3_3](1,3,5)$ CP.

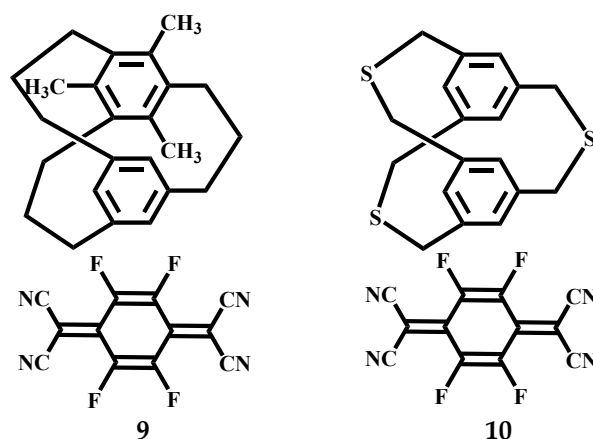


Figure 6. The structures of $\text{Me}_3[3_3]$ CP-, $\text{S}_3[3_3](1,3,5)$ CP-TCNQ-F4 complexes 9 and 10.

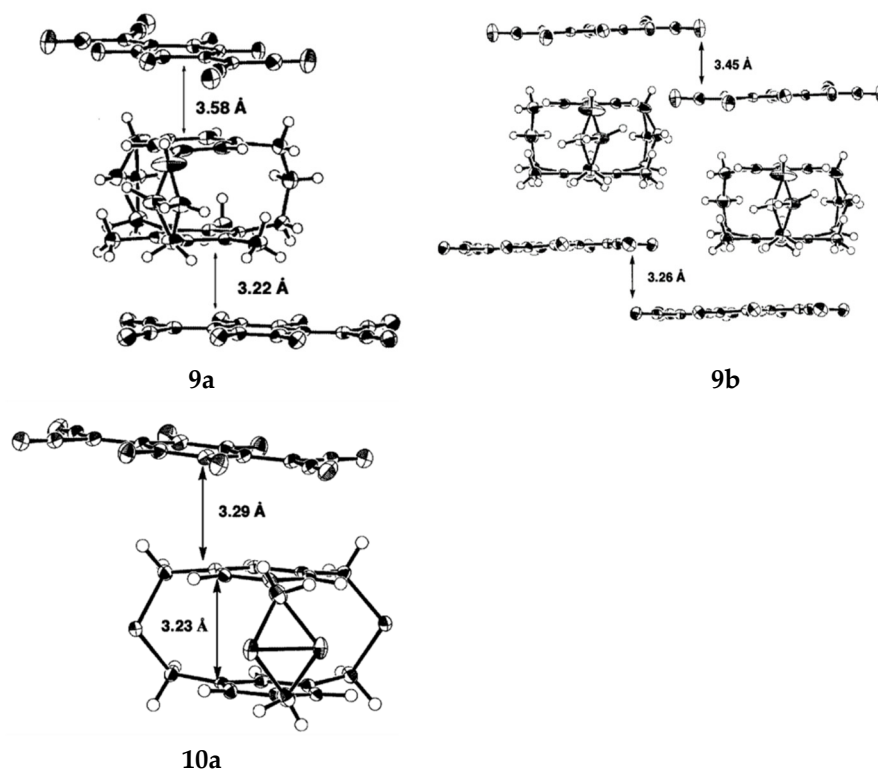


Figure 7. ORTEP drawings of complexes **9** and **10** at $-170\text{ }^{\circ}\text{C}$ (the probability of thermal ellipsoid is 50%).

$[3_3](1, 3, 5)\text{CP}$ **11** observed two conformations with symmetry of C_{3h} and C_s in the ^1H NMR spectrum of 2,2,11,11,20,20-hexa-deuterated in CD_2Cl_2 . **11** (C_s) is more stable than **11** (C_{3h}) by 0.4 kcal/mol. When the bridge is flipped, its energy barrier is 12.4 kcal/mol (Figure 8). The transition state **11** (TS) connecting the C_s and C_{3h} conformations was estimated by density functional calculation (B3LYP) to have only one plane bridge with a dihedral Angle calculated as 180.0° . One of the three bridges can transform conformation independently of the other two bridges. In the solid state, the benzene rings of **11** are completely stacked with a cross-ring distance of 3.08–3.24 Å, resulting in a C_s conformation. Rika et al. studied the photochemical reactions of **11** under a sterilized lamp (254 nm) [56]. In the presence of 2 mol/L aqueous HCl solution, after photolysis in MeOH or CH_2Cl_2 , the cyclophanes $[3_3]$ obtain new caged compounds and produce new skeletons, such as pentacyclo[6.4.0.0.^{3,6}0.^{4,11}0^{5,10}] dodecane skeleton **12**, hexacyclo[6.4.0.0.^{2,6}0.^{4,1}0.^{5,1}0^{9,12}] dodecane **13** and tetracyclo [6.3.1.0.^{2,7}0^{4,11}]dodeca-5,9-diene **14** (Figure 9).

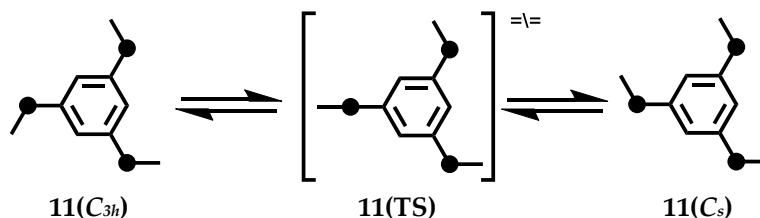


Figure 8. Bridge flipping process and stable conformers of $[3_3](1,3,5)\text{CP}$ **11**.

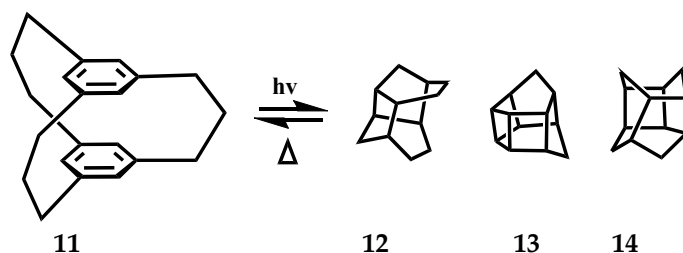


Figure 9. Compound 11 generates a photochemical reaction formula of the new cage compounds 12, 13, and 14 to show only the cage backbone for clarity.

To investigate the structure and cation– π interactions of the metal ion complex, Hiroyuki et al. synthesized a cage-like compound $C_{36}H_{36}S_6$ [57]. In solution, the 1H and ^{13}C NMR spectra showed two or three sharp singlets, respectively, which suggests its symmetrical cage structure. Thus, the inclusive space is satisfyingly retained. However, by crystallographic analysis, the structure of $C_{36}H_{36}S_6$ 15 (Figure 10) in the solid state was not symmetrical but in a collapsed shape (15a). X-ray crystallographic analysis revealed that the compound had a collapsed structure 2,11,20-trithia[3₃](1,3,5)CP 16 (Figure 10).

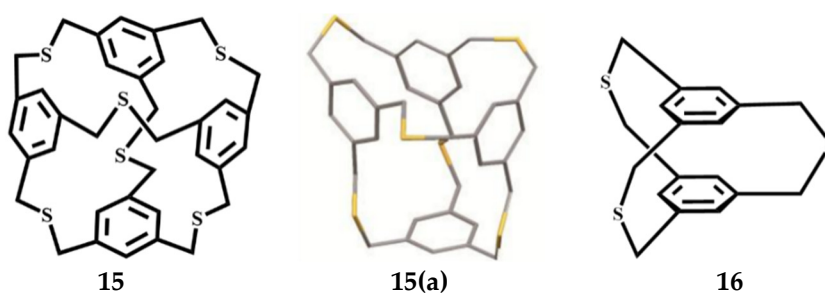


Figure 10. The conformation of $C_{36}H_{36}S_6$ 15 and 2, 11, 20-trithia[3₃](1, 3, 5)cyclophane 16.

Mikio et al. studied the crystal structure of [3₆](1,2,3,4,5,6)CP with a series of complexes synthesized by TCNQ [58]. In the crystal structure of the [3₆](1,2,3,4,5,6)CP-TCNQ-benzene (1:1:1) complex 17 (Figure 11) at -190 °C, a TCNQ (acceptor) and a cyclophane(donor) are stacked together with a D-A distance of 3.30 Å at -190 °C. The benzene ring of cyclophane partially overlaps with the six-membered ring of TCNQ. The short distance (2.64 Å) between an olefinic proton of the TCNQ and a benzene ring suggests the presence of a CH– π interaction. The cyclophane moiety is observed as a D_{6h} conformer, because of the disorder of molecules with a C_{6h} symmetry. The two neighboring cyclophane molecules face in an orthogonal position in the crystals of free [3_n](1,2,3,4,5,6)CP, and this arrangement is generally observed in the crystal structures of [3_n]CP. The cyclophane moiety of the [3₆](1,2,3,4,5,6)CP-TCNQ-F4 (1:1) complex 18 takes the C_{6h} structure in the crystals, the transannular D-A distance is 3.22 Å, the average transannular distance between two benzene rings is 2.93 Å (Figure 11). The complex shows alternating do-nor-acceptor superposition resulting in the partial donor-acceptor overlap. This structural feature can be explained by the orbital interaction between the acceptor LUMO and the donor HOMO.

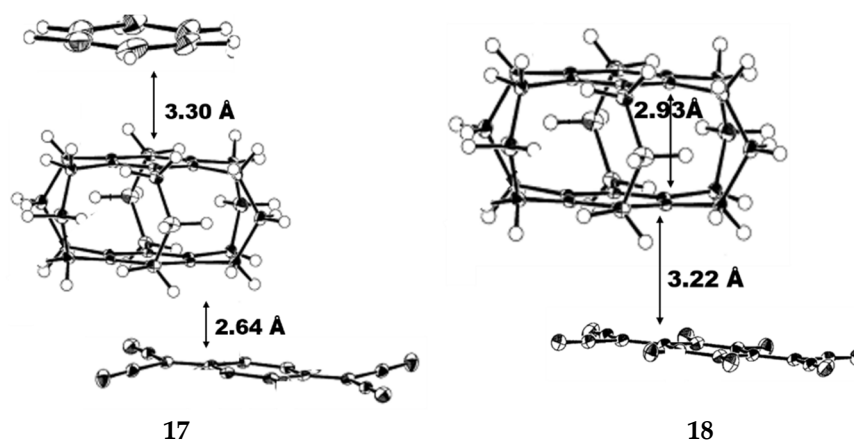


Figure 11. ORTEP drawings of complexes **17** and **18** at $-190\text{ }^{\circ}\text{C}$ (the probability of thermal ellipsoid is 50%).

Koga et al. synthesized trifluoro- and hexafluoro $[3_3](1,3,5)$ CP **19**, **20** (Figure 12) and studied their crystal structure [59]. Their structures exist in the C_s conformation in the crystalline state, and the molecules can be stacked face-to-face with the fluorinated benzene ring to form a column. In all nonfluorinated $[3_n]$ CPs ($n = 3-6$), the two neighboring molecules are perpendicular, which is a structural feature of fluorinated derivatives. Therefore, the H-F class hydrogen bond interaction is more significant in **20** than in **19**. The longest $\pi-\pi^*$ absorption band shows a blue shift as the number of fluorine atoms increases.

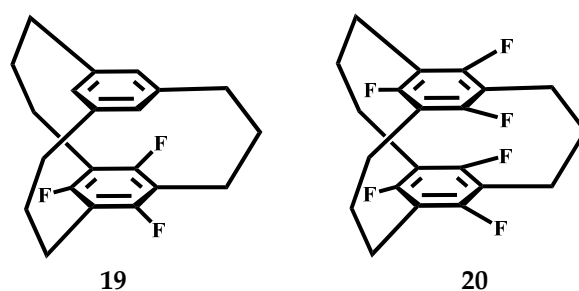
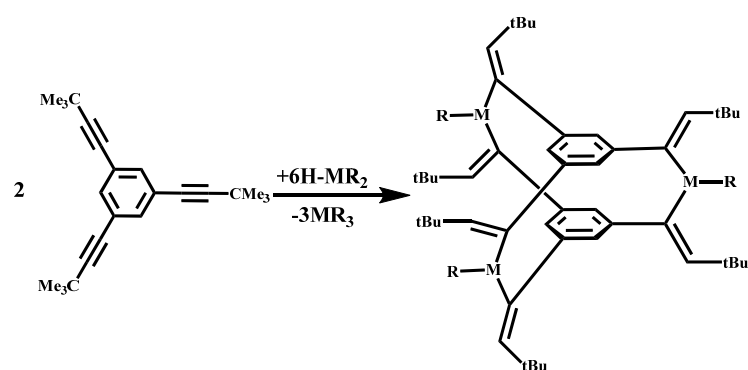


Figure 12. The conformation of Trifluoro- and hexafluoro $[3_3](1,3,5)$ CP **19** and **20**.

2.1.2. Non-Carbon Chain Triple Cage

Werner et al. studied the crystal structure of Aluminum-bridged $[3,3,3]$ cyclophanes, firstly the reaction of 1,3,5-tris(3,3-dimethyl-1-butenyl)benzene $C_6H_3(C\equiv C-CMe_3)_3$ with the dialkyl aluminum hydrides $HAl(CMe_3)_2$ and $HAl(CH_2CMe_3)_2$ gave the addition of one Al-H bond to each C-C triple bond (hydroalumination) [60]. The reaction equation is shown in Figure 13. Spontaneous condensation by the release of the corresponding trialkyl aluminum derivatives afforded $[3,3,3]$ cyclophane derivatives **21** and **22** (Figure 14) in which three tricoordinate Al atoms are in the bridging positions between two functionalized benzene rings. The resonances of the vinylic hydrogen atoms and the protons attached to the aromatic ring are close together and resonate at $\delta = 6.00$ and 6.32 ppm for **21** and $\delta = 6.24$ and 6.22 ppm for **22**. The carbon atoms of the C=C bonds show chemical shifts of $\delta = 152$ and 156 ppm on average; the resonances at higher fields belong to the carbon atoms attached to the phenyl rings and the aluminum atoms. Due to the addition of Al-H bond, the initial $C\equiv C$ bond produces an alkenyl group containing C=C bond, which decreases. The aluminum atom specifically attacks the triple-bonded carbon atom located at the alpha position of the aromatic ring. Hydrogen and aluminum are in cis on the double bond. Trialkylaluminum forms three C-Al-C Bridges between the two aromatic rings, which contain coordinated unsaturated aluminum atoms. The Al-C distance of the terminal alkyl

group is very similar to the Al-C distance of the inner cage. As a result, there was no sign of spatial stress in the cage.



- 21: M=Al, R=CMe₃
 22: M=Al, R=CH₂CMe₃
 23: M=Ga, R=CH₂CMe₃
 24: M=Ga, R=Et
 25: M=Ga, R=nPr

Figure 13. Synthesis of Aluminum-Bridged and Gallium-Bridged [3,3,3] cyclophanes derivatives.

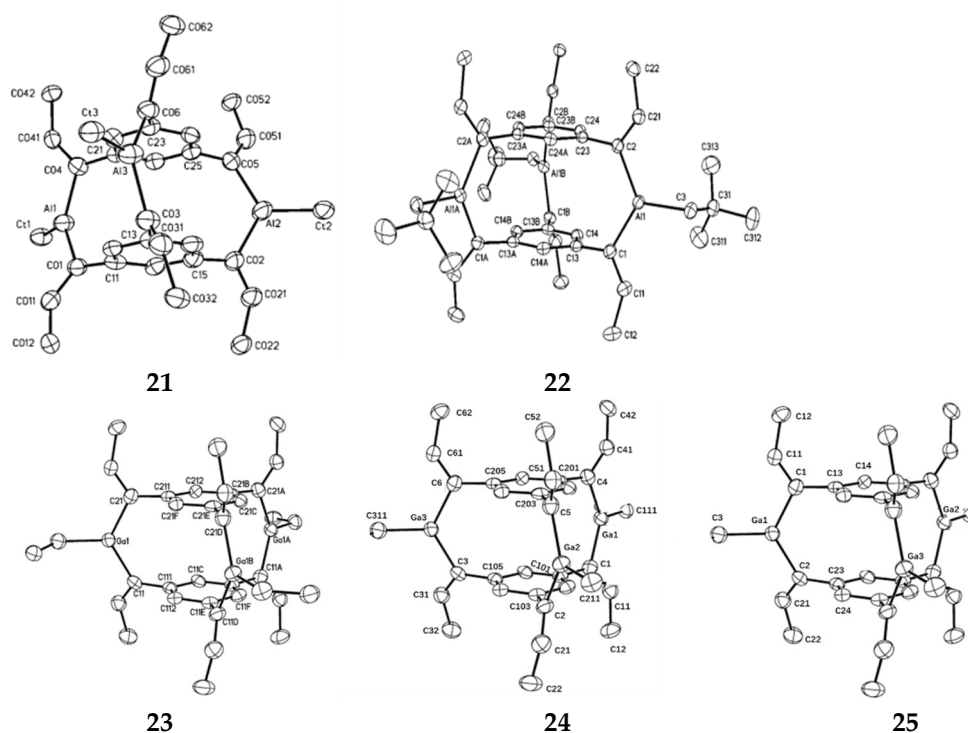


Figure 14. ORTEP drawings of complexes **21**, **22**, **23**, **24**, and **25** (the probability of thermal ellipsoid is 50%).

Werner et al. also report that the reaction of 1,3,5-tris(3,3-dimethyl-1-butynyl)benzene, C₆H₃(C≡C–CMe₃)₃ with di(neopentyl)gallium hydride, HGa(CH₂CMe₃)₂, where each C≡C triple bond add a Ga–H bond (hydration) [61]. A [3,3,3] cyclophane derivative **23** (Figure 14) is generated by spontaneous condensation of tri (neopentyl) gallium, in which three trip coordination Ga atoms are located in bridging positions. The reaction equation is shown in Figure 13, with three carbon atoms bound to gallium atoms on a triangular planar coordination sphere. All configurations on the C=C double bond correspond to the addition of the GA–H bond cis to the alkyne group. Owing to the crystallographic

symmetry, the two benzene rings are coplanar in the ideal state. Instead of the desired overlapping arrangement, they are slightly rotated 4.2° from each other. The R-carbon atom of the C=C double bond deviates only 0.05–0.08 Å from the average plane of the corresponding phenyl group. This small bending of the organic skeleton of a molecule is due to special bonding within the ring-sealed cage. By the reactions of tris(tert-butyl ethyl) benzene with dialkyl gallium hydride Werner et al. also obtained two cyclophane-type molecules **24** and **25** (Figure 14) with three gallium atoms at the bridging position between the two benzene rings [62], the reaction equation is shown in Figure 13. The change in the number of bridge groups does not greatly affect the structural parameters. The C=C double bond length is in good agreement with the standard value, which is about 1.34 Å on average. The C-Ga-C angle in the cage (123°) is slightly increased relative to the ideal value of the sp^2 atom, but this may be due to some strain reaction in the molecule. A larger angle of 131° to 134° was observed for C=C-CMe₃. They may be caused by interactions between the aromatic system and tert-butyl groups, or they may be caused by spatial interactions between tert-butyl groups arranged on a benzene ring.

2.1.3. Triimidazole Bridge Cage

Yi et al. reported the convenient and highly effective synthesis method of novel water-soluble tris-bridged imidazoles containing imidazolium or benzimidazolium groups **26**, **27** (Figure 15) [63]. Analysis by X-ray showed that compound **26** has C_s symmetry. The symmetry mirror is the plane of three 2-C of imidazolium rings. The parallel capping benzene rings are about 5.2 Å apart. The distances of the three 2-C of the imidazolium are 4.5–4.7 Å (Figure 15). The rigidity, size, and shape of cyclophanes **26** and **27** make them suitable for the formation of supramolecular systems containing complex small anions alone.

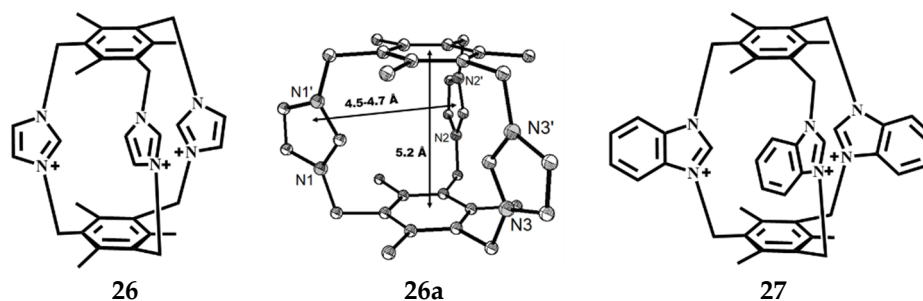


Figure 15. The structures of cyclophanes **26** and **27** and ORTEP drawings of complex **26** (the probability of thermal ellipsoid is 50%).

Yuan et al. obtained a speleand imidazolium cyclophane $[C_{30}H_{33}N_6]^{3+} \cdot 3Br^- \cdot 3H_2O$ **28** by direct quaterization of 1,3,5-trimethyl-2,4,6-tri(imidazolylmethyl) benzene with m-tri(bromomethyl)benzene and its yield is 89% [50], the reaction is shown in Figure 16. The repeating crystal structural unit consists of one large bicyclic triimidazole cyclophane, three bromine anions, and three water molecules. The three imidazole rings and the two benzene rings are surrounded by a cavity, the three imidazole rings are asymmetrically arranged, and there is no symmetry factor in the molecule itself, but the imidazole ring is homogenized, and the positive charge is dispersed on the imidazole ring. Outside the cavity, the nest formed between the imidazole rings can also be used to selectively bind the molecule to anionic or neutral molecules by electrostatic action and cationic 2π interaction. The molecules have a strong rigidity, due to the presence of methylene, the angle between the imidazole rings has a certain degree of tunableness, so that the molecules have a certain large double-ring effect, and can be selectively combined with inorganic, organic anions, or amphoteric and neutral molecules to form a supramolecular system. Preliminary studies have shown that the compound has a good selection and recognition effect on some common anions and polyphenols.

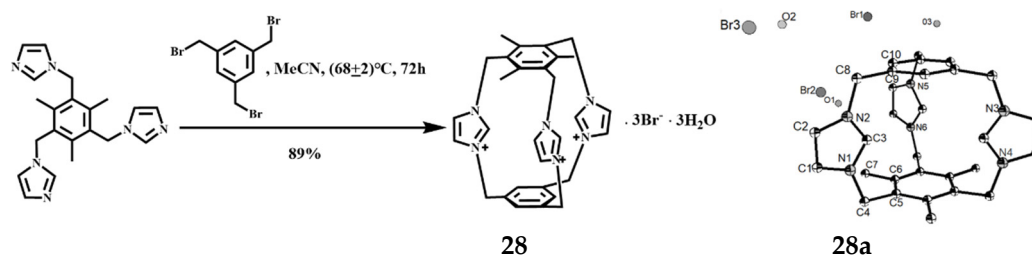


Figure 16. Synthesis and ORTEP drawing of a speleand imidazolium cyclophane **28** (the probability of thermal ellipsoid is 50%).

We synthesized three 3D imidazole or benzimidazole cages **29** (L1·I₃), **30** (L2·I₃), and **31** (L3·Br₂·I) as trivalent cation templates and studied their cage structures (Figure 17). Free asymmetric cage **29** with I[−] only through the weak interaction. Two independent conformations can be found in the crystal structure. The dihedral angles between the benzimidazole rings are 24.53°, 70.44°, and 85.04° in type A, respectively. In type B, the three dihedral angles are 17.03°, 77.25°, and 88.73°, respectively. This indicates that the conformations of the two cages of **29** are different, but they can be changed to some extent. In the structure of asymmetric cage **30**, the two benzene rings are almost parallel, but **30** has a symmetric mirror image, and the plane of symmetry is the plane of the three 2C atoms of the imidazole group. **30** belongs to a class of cylindrical macrocyclic salts containing the imidazole family; the shape of the compound makes it suitable for the formation of exclusive or included complexes with small anions. The structure of **31** is different from that of **30**, which is symmetric, but the size of the cage cavity is similar to that of **30**.

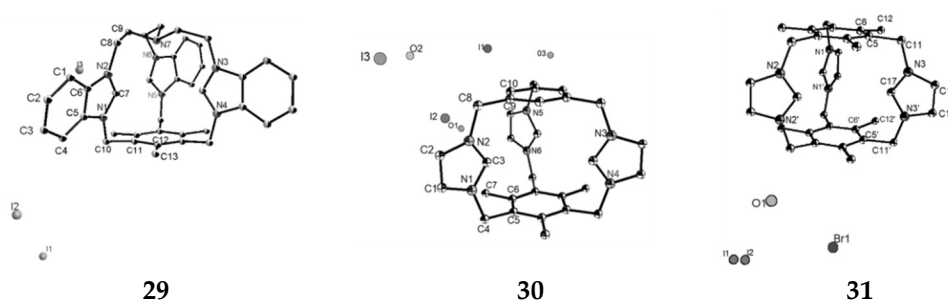


Figure 17. ORTEP drawings of cages **29**, **30** and **31** (the probability of thermal ellipsoid is 50%).

We used **29–31** to assembly with metal (pseudo) halides or molybdates and obtained eight different organic-inorganic supramolecular hybrids: {(L1)₂·[CuBr₃]₃·2(CH₃CN)}**32**, {L1·[CuI₃](H₂O)}**33**, {L2·[PbI₅]}**34**, {(L2)₂·[Cu₂I₅]₂}**35**, {(L3)₂·[CdI₄]₃}**36**, {L3·[HgI₄·I]}**37** {L3·Ag(SCN)₄·(CH₃CN)·2H₂O}**38** and {L2·[HMo₅O₁₇](H₂O)_{3.25}}**39** [64,65], ORTEP drawings are shown in Figure 18. Their structures were determined by single-crystal X-ray diffraction analyses. The structure of compound **32** exhibits conformational contraction and the distance between the benzene ring and the nitrogen atom on ethylamine is 4.909 Å. The dihedral angles of the two benzimidazole rings are 64.93°, 19.70°, and 45.49°, respectively, due to the electrostatic force generated by the cage and the metal halide. **33** and **32** are identical in that the structure consists of **29** and Cu(I) but differ in the anion composition. Due to the hydrogen bond interaction and the electrostatic force between **29** and the metal halide, the vertical height of the cation cage of **33** is shorter than that of the free state **29**. In the structure of compound **34**, the three imidazole rings of the cationic cage are not symmetric, which is attributed to the induction interaction between the cationic cage and [PbI₅]^{3−}, which changes the structure of **34**, resulting in a shorter vertical height of **34** than the free **30**. In the structure of compound **35**, due to the interaction between the cationic cage and the strong Cu–Cu anion in the binuclear cluster species, there are two conformations in **35**, in which the two cationic and anion parts are not the same, resulting

in the benzene ring distance of 5.1905 Å and 5.1415 Å, respectively. These results indicated that the two cages exhibited different breathing behaviors of contraction and expansion. In this structure of compound **36**, the two triimidazole cage cations in the structural unit are different. Different metal halide anions are present in **37** compared with compound **36**. However, the anions in both compounds showed similar compressive effects on the cationic cage. Compound **38** contains strong C–H···N hydrogen bonds, three imidazole rings asymmetrically arranged. In this structure of compound **39**, a stacking pattern formed in the *c* direction due to the action of weak electrostatic forces. In addition, by studying their fluorescence characteristics in the solid state, it is shown that they can be used as fluorescence sensors for detecting Fe³⁺ ions and have high recyclability and sensitivity.

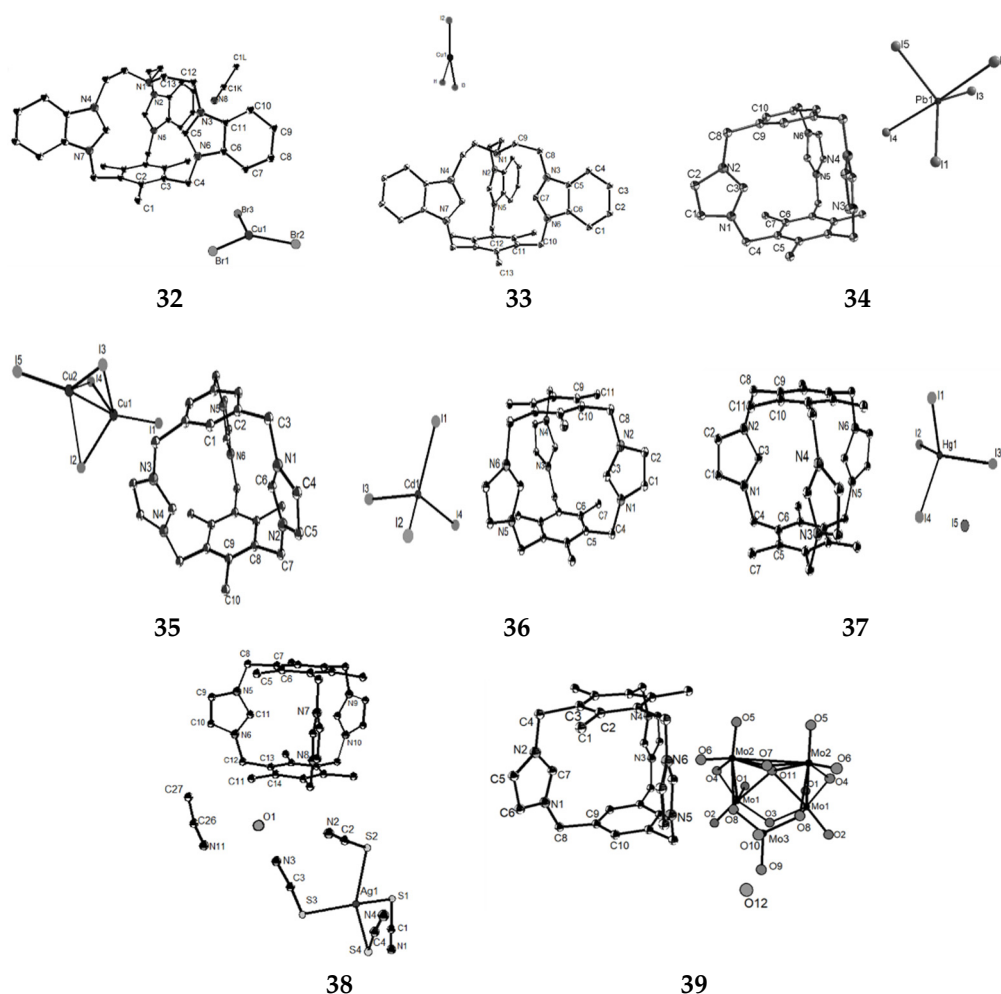


Figure 18. ORTEP drawings of eight different organic-inorganic supramolecular hybrids (the probability of thermal ellipsoid is 50%).

Our previous research has shown that cationic conformations are significant in anion assembly and final architecture [64]. Tris(imidazole) ring cage **29–31** has the characteristics of insufficient internal space and strong rigidity and is looked forward to inhibiting the template effect to induce or contain anionic guests. Mononuclear or polynuclear anionic structures (compounds **32–38**) are generally composed of cationic cages assembled with electron-deficient metal halides. However, when assembled with electron-rich polyoxometalates (POMs), a rare [Mo₅O₁₇]^{4−} anion isomer is produced (compound **39**). Thus, the retention of a 1,3,5-trialkylbenzene cation cap with a special structure may have a typical template effect on electron-rich polyoxometallates. Negatively charged species can also direct the formation of specific molecules and compositions [66]. It is interesting to observe

the triimidazole cage structure from an anionic perspective. Although triimidazole ring cages have a lot to do with anions or anionic clusters, they can only regulate a limited amount of space to accommodate different types of anions. Therefore, the vertical height of the cage can be finely adjusted for the conformation. After complexation with polyoxometalates, the cage-like structure in compound **39** expands (~ 0.07 Å); For metal halides, this complexation leads to shrinkage of the cage (~ 0.01 – 0.1 Å at **32**–**38**) or expansion (~ 0.04 Å at **39**). This mechanism can be described as the “breathing process”. These results show that these rigid cages have certain mobility that is comparable to the conformational changes of the vehicle-pile complexes below (~ 0.16 Å) [67].

Willans et al. reported sterically rigid tris(imidazolium) cyclophane **40** (**L4**) (Figure 19) reacts with Ag_2O to give an Ag(I) mononuclear carbene complex $[\text{Ag}(\text{L4-2H})](\text{PF}_6)_2$ **41** (Figure 19) characterized by X-ray crystallography [68], which revealed a solid-state structure entirely consistent with the solution NMR spectroscopic data. The C–Ag–C angle of the complex is 175.9° , which is linear. The structure exhibits almost perfect specular symmetry, but the slight rotation of the remaining imidazole perpendicular to the C–Ag–C axis breaks the rotation. This change may be attributed to the same resonance of H in acetonitrile, which can be well explained by the detection of NMR spectroscopy, which also shows that the complex is rigid, and the close contact between the Ag(I) central imidazole and CH groups is repulsive, thus increasing the activation barrier of exchange. The centroid separation of the aromatic ring increases from 5.15 Å in the structure of **31** to 5.31 Å due to the axial property of C–Ag–C, which leads to the expansion of the complex. The resulting rigid complex is stable to water and air and exhibits well-defined conformational properties. The reaction of 1,3,5-trimethylimidazole-2,4,6-triethylbenzene with $\text{FeCl}_3 \cdot 6\text{H}_2\text{O}$ in hot water solution resulted in the isolation of **L4** as the mixed bromide–tetrachloroferrate (III) salt, $\text{L4}^{3+}\text{Br}_2 \cdot 2[\text{FeCl}_4]_2$ **42** (Figure 19). Salt **42** adopts a threefold symmetric cubic packing arrangement in the solid state. The molecular structure of the L4^{3+} cation is similar to that of the L3 bromide, although the aromatic intercentroid separation time is shorter (5.08 Å). L4^{3+} and two independent $[\text{FeCl}_4]$ anions are both located on the crystallographic triplet axis, and a chloride ligand penetrates the cage produced by the ethyl substituent to form a very short anion– π interaction with a $\text{Cl}_3\text{Fe-Cl} \cdots \pi$ distance of 3.424 Å, which corresponds to the sum of van der Waals radii. As a result, the triple axis by $\text{L4}^{3+} \cdots [\text{FeCl}_4]_2 \cdots [\text{FeCl}_4]_2 \cdots \text{Br}_2 \cdots \text{L4}^{3+}$ polarity chain as the packing, etc. The addition of Br^- allows the structure to avoid the mismatch between the cyclomatic hydrocarbon and the triangular face of the $[\text{FeCl}_4]$ anion. That is, bromine incorporation is necessary because the cation has an amorphous mirror symmetry perpendicular to the triple axis of the molecule and the crystal, whereas the tetrahedral anion does not. This co-existence of highly symmetric matching and hindrance provides a possible strategy for the design of polar molecular crystals.

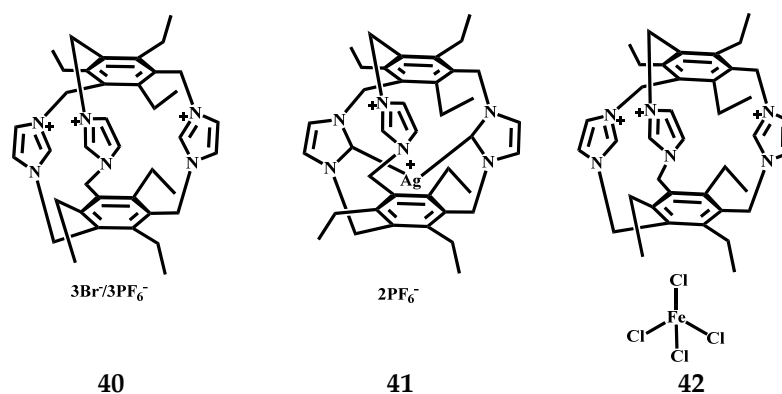


Figure 19. The structures of tris(imidazolium) cyclophane **40** and its two organic-inorganic supramolecular hybrids.

2.2. Crystalline Four-Fold Bridged Cyclophanes

Mikio et al. estimated by Molecular Orbital calculations that the most stable conformation of $[3_4](1,2,3,5)CP$ crystals at $-150\text{ }^\circ\text{C}$ is the C_s structure. The transannular distance between the two benzene rings of cyclophane is $3.198\text{--}2.978\text{ \AA}$ [37]. The distance between $C4\text{--}C4'$ without bridge (3.198 \AA) is much longer than that between $C1\text{--}C1'$ with bridge (2.978 \AA) (Figure 20). These data illustrate certain variations of the benzene rings of $[3_4](1,2,3,5)CP$. In addition, $[3_4](1,2,3,5)CP\text{-TCNQ-F4}$ (1:1) complex **43** (Figure 20) shows the C_s structure in the crystal. The crystal structure of pseudogemstone-acetylformyl $[3_4](1,2,3,5)CP$, a significant synthetic intermediate in aldol reaction, was also determined. The benzene ring was perpendicular to the attached acetyl group, the formyl group was located in the plane of the attached benzene ring, and the carbonyl oxygen was oriented to the inner side of the molecule. In bright comparison to the molecular structures of the monoacetyl compound 5-acetyl $[3_4](1,2,4,5)CP$ **44** and the diacetyl compound 5,18-diacetyl $[3_4](1,2,4,5)CP$ **45**, the two benzene rings are completely stacked in pseudogem-acetylformyl $[3_4](1,2,4,5)CP$ **46** (Figure 20).

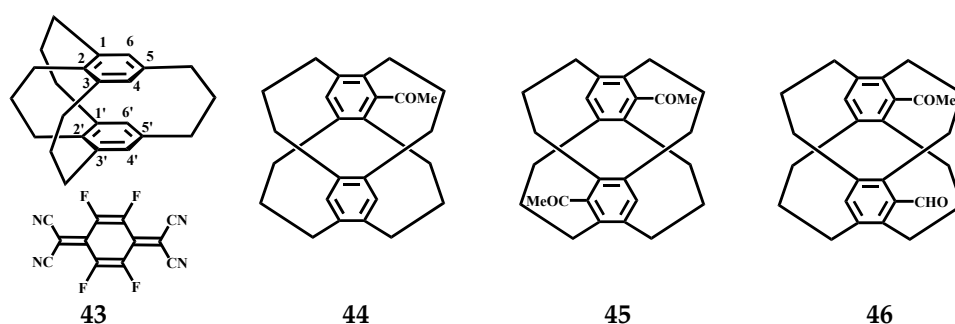


Figure 20. The structures of $[3_4]CP\text{-TCNQ-F4}$ complex **43** and the monoacetyl and diacetyl compounds **44**, **45** and **46**.

Wakana et al. reported the modified synthetic route to $[3_4](1,2,4,5)CP$ **47** provide gram quantities of this compound in fewer steps than the conventional routes [69]. The cycloaddition of $[3_4](1,2,4,5)CP$ with dicyanoacetylene gave barrelenophane **48**, which was transformed into semibullvalenophane **49** on photoirradiation, the reaction formula is shown in Figure 21. The X-ray structural analyses of **47**, **48**, and **49** demonstrate their unique structures. The geometry of the benzene ring of **47** is bent from planar to a boat-shaped form, the molecule assumes the most stable D_{2h} structure. In the structural diagram of barrelenophane **48**, four trimethylene bridges assume the boat–boat conformation, and a similar boat-shaped deformation of the benzene ring was also found. Tetra-bridge cyclohexanol **48** has a low strain and rigid structure. Compound **49** is the structure of the semibullvalenophane, the benzene ring of **49** is slightly deformed into the boat form and the distortion angle α is 9.89° . The cyclopropane ring of **49** is significantly distorted from a regular triangle.

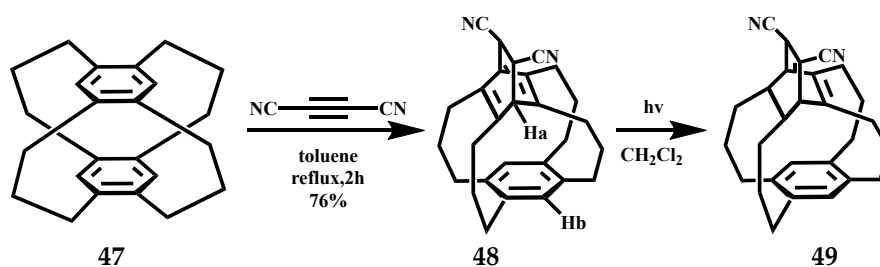


Figure 21. The cycloaddition and photoirradiation of $[3_4](1,2,4,5)CP$ **47**.

Toshiaki et al. have examined the coupling conditions of tetrabromide with three kinds of tetrasubstituted durene derivatives, to optimize the synthesis method of tetrathiacyclophanes **50** and **51** [70], the reaction formula is shown in Figure 22. Compound **50** shows a D_{2h} symmetric isomer and compound **51** shows a C_{2v} symmetric isomer in the crystal structures. Their structural diagram shows four $-\text{CH}_2\text{-S-CH}_2\text{-}$ bridge conformations, in which all the sulfur atoms point to the unsubstituted aromatic hydrogen. The two rings may slide in parallel to reduce repulsive forces.

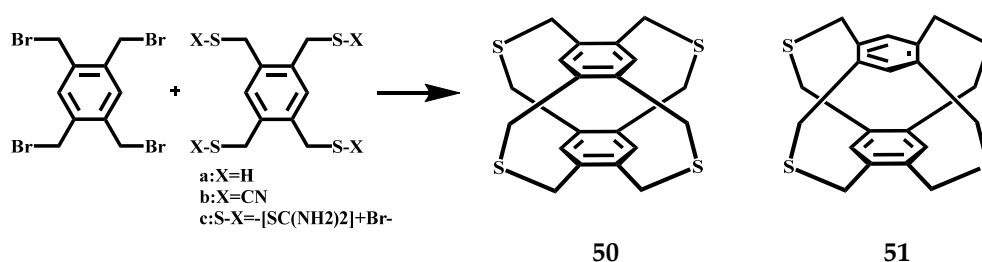


Figure 22. Synthesis of tetrathiacyclophanes **50** and **51**.

Stefan et al. cyclized the quadruple functionalized cyclophane **52** with the toxamide monosodium salt to obtain a new quadruple bridged cyclophane **53** [71], the reaction formula is shown in Figure 23. The crystal structures of **52** and **53** were analyzed by X-ray. Although the structure of **52** contains four bromomethyl groups, it still shows a typical cyclophane conformation. Two of the bromomethyl groups point into the interior of the cyclophane, which is caused by crystal packing. In addition, the zig-zag arrangement of cyclophanes in the crystal structure may be due to intermolecular bromine–bromine interactions. Each **53a** structure contains a molecule of trichloromethane, and each host molecule forms a hydrogen bond with a sulfonyl group. The phenyl propyl group and the second phenyl propyl group of the adjacent molecule will form an H bond and have a weak interaction. The conformation of the first nitrogenous bridge forming the hydrogen bond is ship–ship, while the second nitrogenous bridge is chair-shaped and positively intersected with the cyclophane skeleton. Crystal **53b** was obtained from the toluene solution, and each host molecule contained two solvent molecules. The first toluene molecule acted as a tweezer and formed X-donor through CH–X interaction. The other toluene molecule plays the role of inclusion and does not bind to other molecules. It exists between the two crystal layers and shows weak interaction with the cyclophane molecules in each layer. X-ray analysis showed that the crystallization of **53** in two different solvents resulted in a conformational change in the guest, with crystal **53a** containing trichloromethane having a boat conformation with a C_s symmetry, whereas crystal **53b** containing toluene had a chair conformation with a C_{2v} symmetry. Through a structural comparison of the two, it was found that different sizes and types of molecular bands and molecular tubes could be obtained by changing the building blocks in the synthesis strategy.

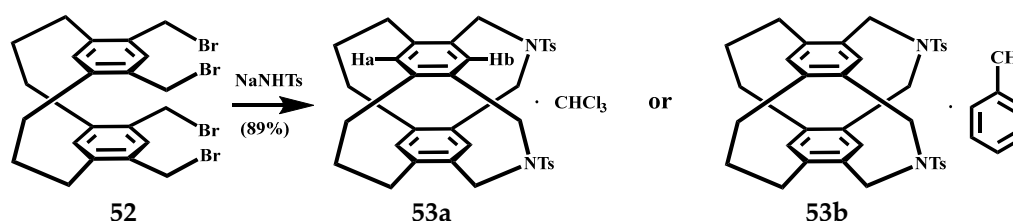


Figure 23. Synthesis of a new quadruple bridged cyclophane **53**.

Josten et al. prepared the fourfold-bridged cyclophane **54** by intramolecular and intermolecular cyclization reactions [72], the reaction formula is shown in Figure 24. The X-ray structure analyses of **54** show S-shaped conformations of the molecules. By analyzing

its single crystal structure, studied the crystallization of Aza[3.3]-supercyclone in a synchronous conformation and had a characteristic sequence of boat/armchair conformations in bridges.

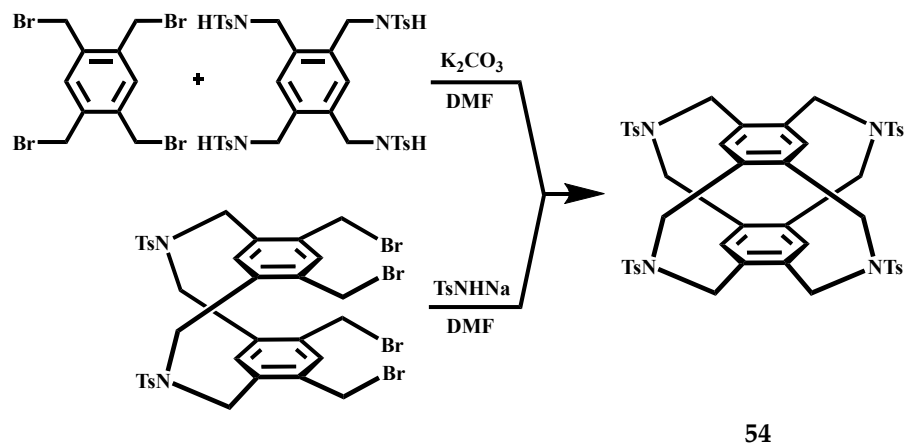


Figure 24. Synthesis of the fourfold-bridged cyclophane **54**.

2.3. Crystalline Five-Fold Bridged Cyclophanes

Mikio et al. studied the structure of $[3_5](1,2,3,4,5)CP$ **55**, as shown in Figure 25, **55b** is the most stable conformation of the three $[3_5]CP$ s [37]. At $-180\text{ }^\circ\text{C}$, in the crystal structure of the $[3_5]CP$ -TCNQ (1:1) complex **56**, its D-A distance is 3.25 \AA (Figure 26), complex **57** (2:1) and $[3_6](1,2,3,4,5,6)CP$ -TCNQ-F4 (1:1) complex **18** similar to that of D-A overlapping structure. The distance between the acceptors in the unit cell is 3.42 \AA (Figure 26). The cyclophane structure of CP-TCNQ adopts the C_s conformation, and the disorder of the bridge is observed, which is related to the semblable stability of **55a** and **55b** conformations. The enone bridge of **58** (Figure 27) has a planar structure, and the two adjacent trimethyl bridges are far away from the enone bridge. $[3_5](1,2,3,4,5)$ -CP-1-one **59** (Figure 27) crystal structure is similar to $[3_5]CP$ **55**. The cross-ring distance between the benzene carbon and the $COCH_2CH_2$ - group was 2.93 \AA , which was shorter than the other distances (3.05 and 3.22 \AA).

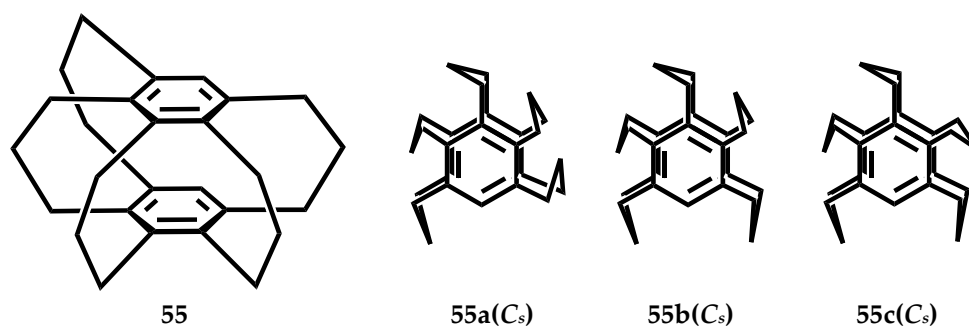


Figure 25. The stable conformers of **55a**, **55b** and **55c** of the $[3_5]CP$ **55**.

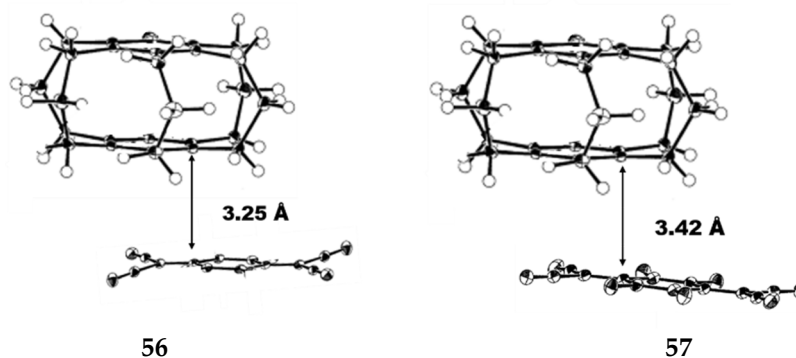


Figure 26. ORTEP drawings of complex 56 and 57 at $-180\text{ }^{\circ}\text{C}$ (the probability of thermal ellipsoid is 50%).

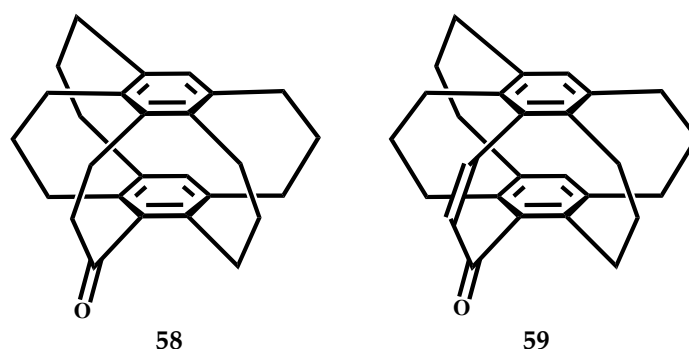


Figure 27. The structures of $[3_5](1,2,3,4,5)\text{CP-1-one}$ 58 and 59.

2.4. Crystalline Six-Fold Bridged Cyclophanes

Mikio et al. studied the structure of $[3_6](1,2,3,4,5,6)\text{CP}$. On the one hand, in the crystal structures of the $[3_6](1,2,3,4,5,6)\text{CP-TCNQ}$ (1:1) complex 17 (Figure 11) exhibits molecular disorder with C_{6h} symmetry, while its cyclophane fraction is observed to be D_{6h} structure [37]. On the other hand, the C_{6h} structure is observed in the crystal of $[3_6](1,2,3,4,5,6)\text{CP-TCNQ-F4}$ (1:1) complex 18 (Figure 11), which showed alternating donor-acceptor superposition and partial donor-acceptor overlap.

3. Conclusions

In summary, the conformational behavior of the four types of crystalline multiple-bridged cyclophanes: three-fold bridged cyclophanes, four-fold bridged cyclophanes, five-fold bridged cyclophanes and six-fold bridged cyclophanes is enumerated. By changing the type of aromatic compounds or regulating the type and quantity of bridging groups, multiple-bridged cyclophane cages are endowed with new self-assembly strategies and physical-chemical properties. The elongation of the bridge makes the cyclophane structure more strain-free and more flexible. It is shown that $[3_n]\text{CPs}$ have a stronger π -electron delivery capability than the corresponding $[2_n]\text{CPs}$. The crystallization of cyclophane from different solvents may lead to guest-dependent conformational variations. By using $[3_n]\text{CPs}$ with strong power supply capabilities, they can be used as electron donors and electron receptors such as TCNE, TCNQ, and TCNQ-F4, so $[3_n]\text{CPs}$ may be donor molecular candidates with great promise for the development of new conductive electronic materials, which is of great significance for the development of electronic conductors and superconductors.

Due to the presence of flexible alkylene bridges, the multiple-bridged molecule has strong rigidity/tunableness and can be selectively combined with inorganic, organic anion, or neutral molecule/atom to form a supramolecular host-guest system. For example, a multiple-bridged cyclophane cage consisting of benzene rings and positively charged

imidazole rings can form a cavity that encapsulates some suitably sized anions. Outside the cavity, the nests formed between the imidazole rings can also be used to selectively bind the molecule to anionic or neutral molecules by electrostatic action and cationic- π interaction; whereas inserting a noble gas (Ng) atom into the cavity of the superphane molecule [2.2.2.2.2](1,2,3,4,5,6)cyclophane with six flexible ethylene bridges may lead to the formation of a Ng@superphane endohedral complex and the corresponding significant “swelling”, which is mainly manifested by increasing the distance between benzene rings [73].

The study of these crystalline multi-bridge cyclophanecages not only provides interesting examples of chemical conformations, but also provides new insights into the construction of functional solid materials. At the same time, the effects of host structure modification and different guests on the obtained supramolecular structure can be evaluated, the mechanism of host-guest framework formation can be elucidated, and the potential application of its structure-performance relationship as functional materials can be further explored.

Author Contributions: Conceptualization, X.-X.Z., J.L. and Y.-Y.N.; methodology, X.-X.Z., J.L. and Y.-Y.N.; investigation, X.-X.Z., J.L. and Y.-Y.N.; resources, X.-X.Z., J.L. and Y.-Y.N.; writing—original draft preparation, X.-X.Z., J.L. and Y.-Y.N.; writing—review and editing, X.-X.Z., J.L. and Y.-Y.N.; visualization, X.-X.Z., J.L. and Y.-Y.N. All authors have read and agreed to the published version of the manuscript.

Funding: This research received no external funding.

Institutional Review Board Statement: Not applicable.

Informed Consent Statement: Not applicable.

Data Availability Statement: Not applicable.

Acknowledgments: The author would like to thank Niu Yunyin of College of Chemistry, Zhengzhou University for his guidance. All individuals included in this section have consented to the acknowledgement.

Conflicts of Interest: The authors declare no conflict of interest.

Sample Availability: Samples of the compounds are not available from the authors.

References

1. Amabilino, D.B.; Gale, P.A. Supramolecular chemistry anniversary. *Chem. Soc. Rev.* **2017**, *46*, 2376–2377. [[CrossRef](#)] [[PubMed](#)]
2. Kolesnichenko, I.V.; Anslyn, E.V. Practical applications of supramolecular chemistry. *Chem. Soc. Rev.* **2017**, *46*, 2385–2390. [[CrossRef](#)] [[PubMed](#)]
3. Zhang, L.-X.; Zhao, W.-X.; Yang, Q. Flourishing development of cyclophane chemistry. *Appl. Chem. Ind.* **2011**, *40*, 1081–1084.
4. Izatt, R.M.; Charles, J. Pedersen’s legacy to chemistry. *Chem. Soc. Rev.* **2017**, *46*, 2380–2384. [[CrossRef](#)] [[PubMed](#)]
5. Ollerton, K.; Greenaway, R.L.; Slater, A.G. Enabling technology for supramolecular chemistry. *Front. Chem.* **2021**, *9*, 774987. [[CrossRef](#)]
6. Misturini, A.; Ortolan, A.O.; Caramori, G.F.; Cintra, C.H.; Parreira, R.L.T. Tracking the absence of anion- π interactions in modified [2₃](1,3,5)cyclophanes: Insights from computation. *New J. Chem.* **2019**, *43*, 13271–13281. [[CrossRef](#)]
7. McConnell, A.J.; Haynes, C.J.E.; Caltagirone, C.; Hiscock, J.R. Supramolecular chemistry: Young talents and their mentors. *ChemPlusChem* **2020**, *85*, 2544–2545. [[CrossRef](#)]
8. He, G.-Y.; Sun, X.-Q.; Wang, X. Properties, applications and synthesis of cyclophane-like tetracation cyclobis(paraquat-p-phenylene). *Chin. J. Org. Chem.* **2004**, *24*, 745–752.
9. Andrea, B.B.; Mohamed, N.; Andreas, H. Supramolecular chemistry in the biomembrane. *ChemBioChem* **2020**, *21*, 886–910.
10. Lu, D.P.; Huang, Q.; Wang, S.D.; Wang, J.Y.; Huang, P.S.; Du, P.W. The supramolecular chemistry of cycloparaphenylenes and their analogs. *Front. Chem.* **2019**, *7*, 668. [[CrossRef](#)]
11. Ewa, W.W.; Łukasik, N.; Biernat, J.F.; Luboch, E. Azo group(s) in selected macrocyclic compounds. *J. Incl. Phenom. Macrocycl. Chem.* **2018**, *90*, 189–257.
12. Zhong, D.-C.; Lu, T.-B. Molecular recognition and activation by polyaza macrocyclic compounds based on host-guest interactions. *Chem. Commun.* **2016**, *52*, 10322–10337. [[CrossRef](#)] [[PubMed](#)]
13. Gulder, T.; Baran, P.S. Strained cyclophane natural products: Macrocyclization at its limits. *Nat. Prod. Rep.* **2012**, *29*, 899–934. [[CrossRef](#)]

14. Ghasemabadi, P.G.; Yao, T.-G.; Bodwell, G.J. Cyclophanes containing large polycyclic aromatic hydrocarbons. *Chem. Soc. Rev.* **2015**, *44*, 6494–6518. [[CrossRef](#)] [[PubMed](#)]
15. Shul'pin, G.B.; Rybinskaya, M.I. Ferrocenophanes. *Russ. Chem. Rev.* **1974**, *43*, 716. [[CrossRef](#)]
16. Neira, I.; Blanco-Gómez, A.; Quintela, J.M.; García, M.D.; Peinador, C. Dissecting the “Blue box”: Self-assembly strategies for the construction of multipurpose polycationic cyclophanes. *Acc. Chem. Res.* **2020**, *53*, 2336–2346. [[CrossRef](#)]
17. Liu, W.-Q.; Johnson, A.; Smith, B.D. Guest back-folding: A molecular design strategy that produces a deep-red fluorescent host/guest pair with picomolar affinity in water. *J. Am. Chem. Soc.* **2018**, *140*, 3361–3370. [[CrossRef](#)]
18. Patricia, R.C.; Rolando, L.G.; Aaron, T.H.; Margarita, B.U.; Victor, B.; Herbert, H. On the organizing role of water molecules in the assembly of boronic acids and 4,4'-bipyridine: 1D, 2D and 3D hydrogen-bonded architectures containing cyclophane-type motifs. *Cryst. Growth Des.* **2009**, *9*, 1575–1583.
19. Li, Y.-Y.; Wang, F.-R.; Li, Z.-Y.; Yan, Z.-N.; Niu, Y.-Y. Assembly and Adsorption Properties of Seven Supramolecular Compounds with Heteromacrocyclic Imidazolium. *ACS Omega* **2019**, *4*, 8926–8934. [[CrossRef](#)]
20. Dale, E.J.; Vermeulen, N.A.; Juriček, M.; Barnes, J.C.; Young, R.M.; Wasielewski, M.R.; Stoddart, J.F. Supramolecular explorations: Exhibiting the extent of extended cationic cyclophanes. *Acc. Chem. Res.* **2016**, *49*, 262–273. [[CrossRef](#)]
21. Malgorzata, D.; Anna, N.Z.; Wanda, S. Radical-radical rotaxanes with tetracationic cyclophane ring, and quaternary azaaromatic rotaxanes with cage macrocycles. *Arkivoc* **2014**, *2014*, 264–306.
22. van Eis, M.J.; Seiler, P.; Muslinkina, L.A.; Badertscher, M.; Pretsch, E.; Diederich, F.; Alvarado, R.J.; Echegoyen, L.; Nunez, I.P. Supramolecular fullerene chemistry: A comprehensive study of cyclophane-type mono- and bis-crown ether conjugates of C-70. *Helv. Chim. Acta* **2002**, *85*, 2009–2055. [[CrossRef](#)]
23. Yu, G.C.; Chen, X.Y. Host-guest chemistry in supramolecular theranostics. *Theranostics* **2019**, *9*, 3041–3074. [[CrossRef](#)] [[PubMed](#)]
24. Cherenok, S.O.; Miroshnichenko, S.I.; Drapailo, A.B.; Kalchenko, O.I.; Rodik, R.V.; Boiko, V.I.; Matveev, Y.I.; Ruban, A.V.; Kalchenko, V.I. Supramolecular chemistry of phosphorus-containing (thia) calixarenes. *Phosphorus Sulfur Silicon Relat. Elem.* **2011**, *186*, 878–883. [[CrossRef](#)]
25. Foster, J.A.; Steed, J.W. Exploiting cavities in supramolecular gels. *Angew. Chem. Int. Ed. Engl.* **2010**, *49*, 6718–6724. [[CrossRef](#)]
26. Beyeh, N.K.; Nonappa Liljestrom, V.; Mikkila, J.; Korpi, A.; Bochicchio, D.; Pavan, G.M.; Ikkala, O.; Ras, R.H.A.; Kostianen, M.A. Crystalline cyclophane-protein cage frameworks. *ACS Nano* **2018**, *12*, 8029–8036. [[CrossRef](#)]
27. Faust, R. Fullerene model compounds: Bowl-shaped aromatic hydrocarbons and cyclophane-based cage molecules. *Angew. Chem. Int. Ed. Engl.* **1995**, *34*, 1429–1432. [[CrossRef](#)]
28. Zhao, G.-S.; Liu, W.; Chang, L.-M. Research advances in the synthesis and application of cyclophane. *Chem. World* **2013**, *54*, 118–121.
29. Gleiter, R.; Kratz, D. “Super” Phanes. *Acc. Chem. Res.* **1993**, *26*, 311–318. [[CrossRef](#)]
30. Margherita, D.R.; Pellegrino, L.M.; Carmen, T.; Annunziata, S.; Carmine, G.; Placido, N. Supramolecular organocatalysis in water mediated by macrocyclic compounds. *Front. Chem.* **2018**, *6*, 84.
31. Padnya, P.L.; Wu, X.; Erxleben, A.; Braga, S.S. Editorial: Design of macrocyclic compounds for biomedical applications. *Front. Chem.* **2021**, *9*, 730111. [[CrossRef](#)] [[PubMed](#)]
32. Li, Y.-Y.; Xiao, M.; Wei, D.-H.; Niu, Y.-Y. Hybrid Supramolecules for Azolium-Linked Cyclophane Immobilization and Conformation Study: Synthesis, Characterization, and Photocatalytic Degradation. *ACS Omega* **2019**, *4*, 5137–5146. [[CrossRef](#)] [[PubMed](#)]
33. Zhao, Q.-C.; Miao, L.-C.; Ma, M.-Y.; Liu, L.-J.; Chen, J. Theoretical study on lithiation mechanism of benzoquinone-based macrocyclic compounds as cathode for lithium-ion batteries. *Phys. Chem. Chem. Phys.* **2019**, *21*, 11004–11010. [[CrossRef](#)]
34. Li, Z.-P.; Liu, B.-H. The use of macrocyclic compounds as electrocatalysts in fuel cells. *J. Appl. Electrochem.* **2009**, *40*, 475–483. [[CrossRef](#)]
35. Luo, H.; Chen, L.-X.; Ge, Q.-M.; Liu, M.; Tao, Z.; Zhou, Y.-H.; Cong, H. Applications of macrocyclic compounds for electrochemical sensors to improve selectivity and sensitivity. *J. Incl. Phenom. Macrocycl. Chem.* **2019**, *95*, 171–198. [[CrossRef](#)]
36. Li, P.-F.; Shimoyama, D.; Zhang, N.; Jia, Y.W.; Hu, G.F.; Li, C.L.; Yin, X.D.; Wang, N.; Jäkle, F.; Chen, P. A new platform of B/N-doped cyclophanes: Access to a π -conjugated block-type B₃N₃ macrocycle with strong dipole moment and unique optoelectronic properties. *Angew. Chem. Int. Ed. Engl.* **2022**, *61*, 1–8.
37. Mikio, Y.; Toru, K.; Youichi, S.; Shingo, K.; Ming, Z.; Katsuya, S.; Hitoshi, T.; Satoru, O.; Yoshio, A.; Shinobu, I.; et al. An alternative synthetic route of [3₅](1,2,3,4,5)cyclophane, and structural properties of multibridged [3n]cyclophanes and their charge-transfer complexes in the solid state. *J. Am. Chem. Soc.* **2002**, *124*, 10136–10145.
38. Sakamoto, Y.; Miyoshi, N.; Shinmyozu, T. Synthesis of a “Molecular Pinwheel”: [3.3.3.3.3.3](1,2,3,4,5,6)Cyclophane. *Angew. Chem. Int. Ed. Engl.* **1996**, *35*, 549–550. [[CrossRef](#)]
39. Sakamoto, Y.; Miyoshi, N.; Hirakida, M.; Kusumoto, S.; Kawase, H.; Rudzinski, J.M.; Shinmyozu, T. Syntheses, Structures, and Transannular π - π Interactions of Multibridged [3n]Cyclophanes. *J. Am. Chem. Soc.* **1996**, *118*, 12267–12275. [[CrossRef](#)]
40. Perumal, R.; Muthialu, S. Synthesis of a new class of electron rich chiral cyclophanes with large cavities. *Tetrahedron* **2003**, *59*, 5373–5376.
41. Collins, M.S.; Phan, N.-M.; Zakharov, L.N.; Johnson, D.W. Coupling metalloid-directed self-assembly and dynamic covalent systems as a route to large organic cages and cyclophanes. *Inorg. Chem.* **2018**, *57*, 3486–3496. [[CrossRef](#)] [[PubMed](#)]
42. Morisaki, Y.; Chujo, Y. Cyclophane-containing polymers. *Prog. Polym. Sci.* **2008**, *33*, 346–364. [[CrossRef](#)]

43. Liu, Z.-C.; Nalluri, S.K.M.; Stoddart, J.F. Surveying macrocyclic chemistry: From flexible crown ethers to rigid cyclophanes. *Chem. Soc. Rev.* **2017**, *46*, 2459–2478. [[CrossRef](#)] [[PubMed](#)]
44. Ramaiah, D.; Neelakandan, P.P.; Nair, A.K.; Avirah, R.R. Functional cyclophanes: Promising hosts for optical biomolecular recognition. *Chem. Soc. Rev.* **2010**, *39*, 4158–4168. [[CrossRef](#)]
45. Nozawa, R.; Kim, J.; Oh, J.; Lamping, A.; Wang, Y.; Shimizu, S.; Hisaki, I.; Kowalczyk, T.; Fliegl, H.; Kim, D.; et al. Three-dimensional aromaticity in an antiaromatic cyclophane. *Nat. Commun.* **2019**, *10*, 3576–3577. [[CrossRef](#)] [[PubMed](#)]
46. Yamauchi, Y.; Fujita, M. Self-assembled cage as an endo-template for cyclophane synthesis. *Chem. Commun.* **2010**, *46*, 5897–5899. [[CrossRef](#)]
47. Ferreira, R.B.; Murray, L.J. Cyclophanes as platforms for reactive multimetallic complexes. *Acc. Chem. Res.* **2019**, *52*, 447–455. [[CrossRef](#)]
48. Shad, M.S.; Santhini, P.V.; Dehaen, W. 1,2,3-Triazolium macrocycles in supramolecular chemistry. *Beilstein. J. Org. Chem.* **2019**, *15*, 2142–2155. [[CrossRef](#)]
49. Lan, S.; Ling, L.; Wang, S.Y.; Ma, D. Pillar [5]arene-integrated three-dimensional framework polymers for macrocycle-induced size-selective catalysis. *ACS Appl. Mater. Interfaces* **2022**, *14*, 4197–4203. [[CrossRef](#)]
50. Yuan, Y.; Jiang, Z.-L.; Gao, G.; Yan, J.-M.; Xie, R.-G.; Yu, K.-B. Synthesis and crystal structure of speleand imidazolium cyclophane. *Chem. Res. Chin. Univ.* **2001**, *22*, 412–416.
51. Olivo, G.; Capocasa, G.; Del Giudice, D.; Lanzalunga, O.; Di Stefano, S. New horizons for catalysis disclosed by supramolecular chemistry. *Chem. Soc. Rev.* **2021**, *50*, 7681–7724. [[CrossRef](#)] [[PubMed](#)]
52. Li, G.-W.; Matsuno, T.; Han, Y.; Phan, H.; Wu, S.-F.; Jiang, Q.; Zou, Y.; Isobe, H.; Wu, J.-S. Benzidine/Quinoidal-benzidine-linked, superbenzene-based π -conjugated chiral macrocycles and cyclophanes. *Angew. Chem. Int. Ed. Engl.* **2020**, *59*, 9727–9735. [[CrossRef](#)] [[PubMed](#)]
53. Nakamoto, K.; Urasaki, T.; Hondo, S.; Murahashi, N.; Yonemochi, E.; Terada, K. Evaluation of the crystalline and amorphous states of drug products by nanothermal analysis and Raman imaging. *J. Pharm. Biomed. Anal.* **2012**, *75*, 105–111. [[CrossRef](#)] [[PubMed](#)]
54. Spicer, W.E.; Donovan, T.M. The density of states of crystalline and amorphous Ge and Si. *Phys. Lett.* **1971**, *36*, 459–460. [[CrossRef](#)]
55. Mikio, Y.; Koji, A.; Ming, Z.; Rika, N.; Teruo, S. Solid-state structural study of the charge-transfer complexes of 5,7,9-trimethyl- and 2,11,20-trithia[3₃](1,3,5)cyclophanes. *Eur. J. Inorg. Chem.* **2003**, *2003*, 1343–1351.
56. Rika, N.; Kumi, M.; Minoru, Y.; Takuma, O.; Youichi, S.; Tsutomu, K.; Chultack, L.; Mikio, Y.; Tetsuro, S.; Charles, W.J.; et al. Photochemical study of [3₃](1,3,5)cyclophane and emission spectral properties of [3_n]cyclophanes (n = 2–6). *J. Am. Chem. Soc.* **2004**, *126*, 13732–13741.
57. Hiroyuki, T.; Maiko, N.; Chihiro, K.; Kasumi, T.; Noriko, T.; Yuki, T.; Tetsuo, I. Synthetic study and structure of cage-type cyclophane C₃₆H₃₆S₆. *Tetrahedron Lett.* **2017**, *58*, 1066–1070.
58. Mikio, Y.; Youichi, S.; Satoru, O.; Katsuya, S.; Hitoshi, T.; Teruo, S. Crystal structural properties of a pinwheel compound: [3₆](1,2,3,4,5,6)cyclophane. *Tetrahedron Lett.* **2000**, *41*, 7933–7938.
59. Koga, T.; Yasutake, M.; Shinmyozu, T. Synthesis, electronic spectra, and crystal structural properties of fluorinated [3₃](1,3,5)cyclophanes. *Org. Lett.* **2001**, *3*, 1419–1422. [[CrossRef](#)]
60. Werner, U.; Alexander, H.; Madhat, M.; Andrej, V. Facile synthesis of aluminum-bridged [3,3,3]cyclophanes by hydroalumination. *Eur. J. Inorg. Chem.* **2007**, *2007*, 4133–4137.
61. Werner, U.; Frank, B.; Sima, H.; Friedhelm, R. New insight into hydrogallation reactions: Facile synthesis of a gallium-bridged [3,3,3]-cyclophane. *Organometallics* **2005**, *24*, 2210–2213.
62. Werner, U.; Michael, C.; Sima, H.; Beate, J.; Alexander, H. The reactions of dialkylgallium hydrides with tert-butylethynylbenzenes—A systematic investigation into the course of hydrogallation reactions. *Dalton Trans.* **2007**, *2007*, 417–423.
63. Yi, Y.; Jiang, Z.-L.; Yan, J.-M.; Gao, G.; Albert, S.C.C.; Xie, R.-G. A convenient and effective synthesis of tris-bridged tricationic azolophanes. *Synth. Commun.* **2000**, *30*, 4555–4561.
64. Wang, F.R.; Li, Z.Y.; Wei, D.H.; Niu, Y.Y.; Hou, H.W.; Wu, B.L. The conformational behavior of multivalent tris(imidazolium)cyclophanes in the hybrids with metal (pseudo) halides or polyoxometalates. *CrystEngComm* **2018**, *20*, 7184–7194. [[CrossRef](#)]
65. Zhu, G.-H.; Wang, F.-R.; Wang, W.-X.; Liu, X.-J. Solvo-thermal synthesis of an ultra-sTable 3D luminescent cadmium (II) hybrid and its application as a recyclable luminescent sensor for Fe (III). *Main Group Chem.* **2020**, *19*, 125–138. [[CrossRef](#)]
66. Xu, J.-W.; Lai, Y.-H.; Wang, W.-L. Variable ion selectivity in n.3.3 (13,5)crownphanes: The “Breathing” process. *Org. Lett.* **2003**, *5*, 2781–2784. [[CrossRef](#)]
67. Mitchell, R.H.; Am, J. Conformational Changes of 2,11-Dithia[3,3]metacyclophane. A New Look Using VT NMR and Calculation. *Chem. Soc.* **2002**, *124*, 2352–2357. [[CrossRef](#)]
68. Willans, C.E.; Anderson, K.M.; Junk, P.C.; Barbour, L.J.; Steed, J.W. A small tris(imidazolium) cage forms an N-heterocyclic carbene complex with silver(I). *Chem. Commun.* **2007**, *2007*, 3634–3636. [[CrossRef](#)]
69. Wakana, S.; Teizi, S.; Mikio, Y.; Chultack, L.; Youichi, S.; Tetsuji, I.; Teruo, S. Improved synthesis, structure, and cycloaddition reaction of [3₄](1,2,4,5)cyclophane. *Eur. J. Org. Chem.* **1999**, *1999*, 1223–1231.
70. Toshiaki, A.; Keita, T.; Hiroyuki, H.; Takahiro, K.; Takanori, T.; Masami, S.; Soichi, M. Synthesis and molecular structure of tetrathia[3₄](1,2,4,5)cyclophane. *Chem. Lett.* **1988**, *17*, 417–420.

71. Stefan, B.; Jörg, H.; Susanne, N.; Martin, N.; Kari, R.; Fritz, V. From four-fold functionalised [3.3]cyclophanes to belt-shaped and multibridged molecules. *J. Chem. Soc. Perkin* **1996**, *16*, 2061–2067.
72. Josten, W.; Karbach, D.; Nieger, M.; Vogtle, F.; Hagele, K.; Svoboda, M.; Przybylski, M. Gurtelformige molekule mittels repetitiver synthesestrategie. *Chem. Ber.* **1994**, *127*, 767–777. [[CrossRef](#)]
73. Jabłoński, M. Determining Repulsion in Cyclophane Cages. *Molecules* **2022**, *27*, 3969. [[CrossRef](#)] [[PubMed](#)]